JOURNAL OF CHEMICAL & ENGINEERING DATA

Article

Density, Ultrasonic Velocity, Electrical Conductivity, Viscosity, and Raman Spectra of Methanolic Mg(ClO), Mg(NO), and Mg(OAc) Solutions

Abdul Wahab, and Sekh Mahiuddin

J. Chem. Eng. Data, **2009**, 54 (2), 436-443• Publication Date (Web): 08 October 2008

Density, Ultrasonic Velocity, Electrical Conductivity, Viscosity, and Raman Spectra of Methanolic $Mg(ClO_4)_2$, $Mg(NO_3)_2$, and $Mg(OAc)_2$ Solutions†

Abdul Wahab[‡,§] **and Sekh Mahiuddin***[,‡]

Materials Science Division, North-East Institute of Science and Technology, CSIR, Jorhat - 785 006, Assam, India, and J. Heyrovsky Institute of Physical Chemistry, Academy of Sciences of the Czech Republic, Dolejskova 3, 182 23 Prague 8, Czech Republic

Density, ultrasonic velocity, electrical conductivity, viscosity, and Raman spectra of methanolic $Mg(ClO_4)_2$, $Mg(NO_3)_2$, and $Mg(OAc)_2$ solutions were measured as functions of concentration (dilute to saturation) and temperature ($273.15 \leq T/K \leq 313.15$). The isentropic compressibility, electrical conductivity, and Raman spectral data reveal the following order of anion−solvent interactions and mobility in methanol: $OAc^- < NO_3^- < ClO_4^-$. Anionic effect on the isentropic compressibility and conductivity roughly appear to follow Hofmeister series. Transport properties and Raman spectra also indicate a moderate solvent-shared ion pairing in concentrated $Mg(NO_3)_2$ solutions.

Introduction

Research activities on electrolyte solutions, one of the century old research topics in physical chemistry, received gradual momentum in the 1900s with the advancement of theories and instruments for experimentation. Results vis-à-vis understanding on the solution behavior (dissociation, association, solvation, structure, etc.) of electrolytes in dilute, intermediate, and concentrated regions either in aqueous or nonaqueous medium have been well monographed and reviewed, as time passes, by several authors.[1−20] The solvation structure and properties of electrolyte solutions in aqueous and nonaqueous media have been attracting chemists over the years because of their importance in many areas of science and technology.[6,21] In particular, ion solvation at different concentration regions is a prerequisite for the development of theoretical models to elucidate or predict various solvation phenomena. In a recent paper,[22] we extracted detailed structural information on aqueous $Mg(OAc)_2$ and $Mg(NO_3)_2$ solutions over a wide range of concentrations and temperatures measuring a variety of physicochemical properties like isentropic compressibility, electrical conductivity and viscosity, and Raman spectra in conjunction with molecular dynamics simulations. Here, we extend these measurements to methanolic $Mg(OAc)_2$, $Mg(NO_3)_2$, and $Mg(ClO_4)_2$ solutions. Among the nonaqueous solvents, methanol has extremely good solvent properties for most electrolytes, for instance, adequate liquidous temperature range, moderate dielectric constant, and an extensive hydrogen bonding network.[8,9] Methanol is a potential fuel cell component,[23−25] so its interactions with ions and small molecules is a current issue. Accurate physicochemical and thermodynamic data are also of interest to compare well the general theories of solvation.[26] However, for the present systems, no literature data appear to be available, except for a few conductivity values for $Mg(ClO_4)_2$ at 298.15 K reported in 1945.[27]

In this paper, the density, ultrasonic velocity, electrical conductivity and viscosity, and Raman spectra of methanolic $Mg(OAc)_2$, $Mg(NO_3)_2$, and $Mg(ClO_4)_2$ solutions over wide range of concentrations and temperatures are reported. The measured data in terms of ion−solvent and ion−ion interactions and possible anionic Hofmeister effects are discussed.

Experimental

$Mg(OAc)_2 \cdot 4H_2O$ (> 99 % SRL, India), $Mg(NO_3)_2 \cdot 6H_2O$ (> 99 %, s.d. fine-chem, India), and $Mg(ClO_4)_2 \cdot 6H_2O$ (> 98 %, Merck, India) were recrystallized twice from double-distilled water and dried in a vacuum oven at (363.15 to 393.15) K and stored in a vacuum desiccator over P_2O_5. A. R. grade methanol (> 99.5 %, Qualigens Fine Chemicals, India) was further purified as described elsewhere.[28] All the methanolic salt solutions were prepared by mass using the anhydrous methanol. The overall relative uncertainty in the solution preparation was 0.3 %.

The density, ρ, of all the solutions was measured using a graduated pycnometer ($\approx$10 cm^3) with a reproducibility of ± 0.01 %. The pycnometer was calibrated using double-distilled water. For ultrasonic velocity, u, measurement was carried out at 2 MHz using an interferometer (Multifrequency Ultrasonic Interferometer, M83, Mittal Enterprises, India). The interferometer was calibrated with double-distilled water at 298.15 K. The uncertainty in the measurement of ultrasonic velocity was within ± 0.01 %.

The electrical conductivities, κ, of all the solutions were measured at 1 kHz field frequency using platinized platinum electrodes of cell constant = 1.237 cm^{-1} employing four-terminal connections and a higher quality bridge, Precision Component Analyzer 6440A (Wayne Kerr, U.K.). The cell constant was determined by using a 0.1 $mol \cdot kg^{-1}$ aqueous KCl solution at different temperatures,[29] and conductivities of some standard electrolyte solutions were also checked to confirm the cell constant. The viscosity, η, of all the solutions was measured with the help of a Schott-Geräte AVS 310 unit and a Ubbelohde viscometer. Viscometers of cell constants (0.009595 and 0.03004) $mm^2 \cdot s^{-2}$ were used to measure the efflux times in

* Corresponding author. E-mail: mahirrljt@yahoo.com.
† Part of the special issue "Robin H. Stokes Festschrift".
‡ North-East Institute of Science and Technology.
§ Academy of Sciences of the Czech Republic.

10.1021/je800463k CCC: $40.75
Published on Web 10/08/2008

Table 1. Least-Squares Fitted Values of the Constant Parameters of the Density Equation, $\rho = a - b(T/\mathrm{K} - 273.15)$ for Methanolic $Mg(OAc)_2$, $Mg(NO_3)_2$, and $Mg(ClO_4)_2$ Solutions

m/mol·kg^{-1}	a/kg·m^{-3}	b/kg·m^{-3}·K^{-1}	std dev in ρ/kg·m^{-3}
		$Mg(OAc)_2$	
0.0059	812.72 ± 0.14	−0.9738 ± 0.0039	0.06
0.0093	813.68 ± 0.17	−0.9835 ± 0.0048	0.07
0.0140	813.90 ± 0.09	−0.9607 ± 0.0026	0.04
0.0339	815.53 ± 0.13	−0.9616 ± 0.0037	0.05
0.0530	816.80 ± 0.22	−0.9841 ± 0.0063	0.08
0.0646	817.86 ± 0.12	−0.9648 ± 0.0037	0.05
0.0855	818.94 ± 0.21	−0.9863 ± 0.0058	0.08
0.1112	821.42 ± 0.12	−0.9721 ± 0.0037	0.05
0.1402	823.34 ± 0.12	−0.9741 ± 0.0036	0.04
0.1455	824.06 ± 0.29	−0.9822 ± 0.0077	0.10
0.1798	825.84 ± 0.15	−0.9652 ± 0.0042	0.06
0.2003	826.29 ± 0.12	−0.9659 ± 0.0034	0.05
0.2192	827.45 ± 0.11	−0.9796 ± 0.0034	0.04
0.2422	829.57 ± 0.14	−0.9861 ± 0.0041	0.05
0.2668	830.42 ± 0.13	−0.9855 ± 0.0044	0.05
0.3042	831.87 ± 0.20	−0.9798 ± 0.0057	0.08
		$Mg(NO_3)_2$	
0.0082	813.03 ± 0.15	−0.9681 ± 0.0042	0.06
0.0545	818.20 ± 0.14	−0.9661 ± 0.0039	0.05
0.0667	821.22 ± 0.28	−1.005 ± 0.008	0.07
0.1047	824.80 ± 0.20	−0.9647 ± 0.0057	0.08
0.2776	841.37 ± 0.38	−0.9430 ± 0.0104	0.14
0.4024	854.10 ± 0.21	−0.9590 ± 0.0060	0.08
0.4555	858.94 ± 0.36	−0.9603 ± 0.0099	0.12
0.6276	875.82 ± 0.26	−0.9312 ± 0.0073	0.10
0.7820	895.91 ± 0.15	−0.9434 ± 0.0039	0.06
0.8810	896.99 ± 0.23	−0.9191 ± 0.0062	0.10
1.004	910.59 ± 0.12	−0.9210 ± 0.0032	0.05
1.259	938.92 ± 0.23	−0.9461 ± 0.0060	0.09
1.492	959.44 ± 0.23	−0.9053 ± 0.0060	0.10
1.710	977.87 ± 0.15	−0.9094 ± 0.0038	0.06
1.875	989.56 ± 0.27	−0.9379 ± 0.0069	0.10
		$Mg(ClO_4)_2$	
0.0542	818.48 ± 0.27	−0.9588 ± 0.0069	0.10
0.0780	822.81 ± 0.10	−0.9528 ± 0.0033	0.04
0.0925	823.84 ± 0.09	−0.9481 ± 0.0030	0.04
0.1673	833.76 ± 0.20	−0.9575 ± 0.0058	0.09
0.2872	848.10 ± 0.18	−0.9377 ± 0.0052	0.08
0.3228	852.12 ± 0.18	−0.9346 ± 0.0053	0.08
0.4313	867.22 ± 0.36	−0.9333 ± 0.0092	0.14
0.6444	894.15 ± 0.47	−0.9287 ± 0.0119	0.17
1.059	945.85 ± 0.47	−0.8979 ± 0.0117	0.20
1.395	983.09 ± 0.10	−0.8837 ± 0.0025	0.04
1.717	1006.6 ± 0.2	−0.8609 ± 0.0053	0.10
2.000	1031.7 ± 0.3	−0.8488 ± 0.0078	0.10

different concentration regions. At each temperature, five efflux times were averaged to calculate the dynamic viscosity. The uncertainty in the conductivity and the viscosity measurements was within ± 0.4 % and ± 0.5 %, respectively. Thermostat-type Schott-Geräte CT 1450 or Julabo F32 HP was used to maintain a constant temperature of the solutions with ± 0.05 % uncertainty.

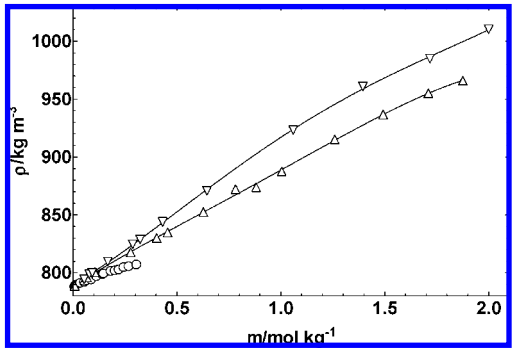

Figure 1. Density vs concentration plots for methanolic ○, $Mg(OAc)_2$; Δ, $Mg(NO_3)_2$; and ∇, $Mg(ClO_4)_2$ solutions at 298.15 K. Symbols are experimental values, and solid curves are calculated from the polynomial equation of the fourth order.

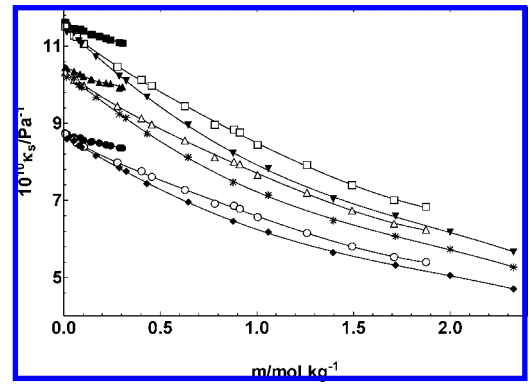

Figure 2. Isentropic compressibility vs concentration plots for methanolic ●,▲,■, $Mg(OAc)_2$; ○,Δ,□, $Mg(NO_3)_2$; and ♦,∗,▼, $Mg(ClO_4)_2$ solutions at ●,○,♦, 273.15 K; ▲,Δ,∗, 298.15 K; and ■,□,▼, 313.15 K. Symbols are experimental, and solid curves are calculated from eq 1.

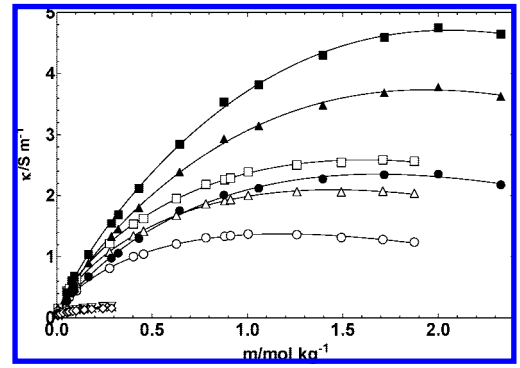

Figure 3. Specific conductivity vs concentration plots at ◇,○,●, 273.15 K; ×,Δ,▲, 298.15 K; and ∇,□,■, 313.15 K for methanolic ◇,×,∇, $Mg(OAc)_2$; ○,Δ,□, $Mg(NO_3)_2$; and ●,▲,■, $Mg(ClO_4)_2$ solutions. Symbols are experimental, and solid curves are calculated from eq 2.

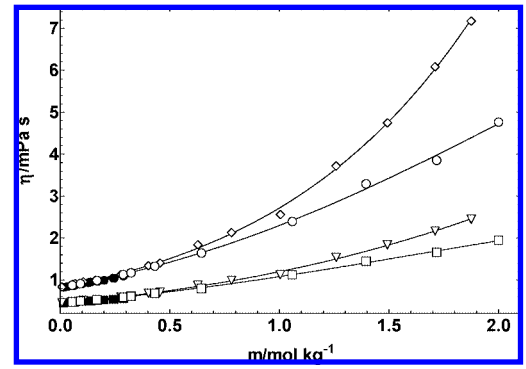

Figure 4. Viscosity vs concentration plots for methanolic ●,■, $Mg(OAc)_2$; ◇,▽, $Mg(NO_3)_2$; and ○,□, $Mg(ClO_4)_2$ solutions at ●,◇,○, 273.15 K; and ■,▽,□, 313.15 K. Symbols are experimental, and solid curves are calculated from eq 3.

FT-Raman spectra were recorded at room temperature from a Bruker IFS 66 V optical bench having an FRA 106 Raman module. A 1064 nm light source from a Nd:YAG laser was used for excitation. Laser power was fixed at 200 mW, and 250 averaged scans were collected with a resolution of 2 cm^{-1}. The spectra were recorded at the SAIF, Indian Institute of Technology-Madras, India.

Results and Discussion

Density. The measured densities for methanolic $Mg(OAc)_2$, $Mg(NO_3)_2$, and $Mg(ClO_4)_2$ solutions are collected in Table 1S (Supporting Information) and are summarized in Table 1 in the

Table 2. Ultrasonic Velocity, u/m·s^{-1}, of Methanolic $Mg(OAc)_2$, $Mg(NO_3)_2$, and $Mg(ClO_4)_2$ Solutions As Functions of Concentration and Temperature

m	T/K										
mol·kg^{-1}	273.15	278.15	283.15	288.15	293.15	298.15	303.15	308.15	313.15	318.15	323.15
						$Mg(OAc)_2$					
0.0059	1185.9	1169.1	1152.8	1135.7	1119.0	1102.5	1086.1	1070.1	1053.9		
0.0093	1186.1	1169.4	1153.2	1136.1	1118.9	1102.0	1085.4	1068.7	1054.5		
0.0180	1186.2	1170.0	1154.7	1137.4	1120.9	1103.5	1086.1	1071.5	1055.7		
0.0530	1190.2	1172.6	1156.3	1138.1	1121.1	1104.6	1087.5	1075.1	1059.6		
0.0855	1190.1	1176.6	1156.5	1139.7	1122.8	1106.7	1090.3	1073.8	1059.0		
0.1024	1194.5	1176.8	1160.3	1142.7	1126.0	1109.8	1093.3	1077.1	1061.0		
0.1402	1194.6	1177.7	1160.4	1144.3	1128.4	1111.6	1092.4	1078.5	1062.7		
0.1455	1192.6	1175.0	1158.5	1141.6	1124.4	1108.4	1091.9	1075.3	1059.1		
0.1837	1195.3	1179.3	1161.7	1143.8	1127.3	1110.9	1094.3	1078.1	1061.4		
0.2192	1196.7	1181.0	1162.8	1147.5	1130.4	1113.4	1097.7	1081.5	1064.3		
0.2422	1196.9	1179.9	1163.1	1146.4	1129.6	1112.7	1095.1	1081.2	1064.9		
0.2889	1197.1	1180.9	1163.5	1147.0	1131.7	1115.2	1098.2	1082.0	1066.1		
0.3042	1199.6	1181.7	1165.8	1149.4	1132.6	1116.1	1099.8	1083.6	1067.2		
						$Mg(NO_3)_2$					
0.0082	1187.6	1171.2	1158.5	1141.9	1123.3	1108.5	1091.9	1075.4	1059.8	1044.1	1027.3
0.0545	1194.3	1178.6	1163.6	1145.7	1129.0	1115.7	1098.1	1082.1	1066.6	1045.1	1033.4
0.0667	1197.6	1181.3	1164.3	1147.2	1130.5	1113.6	1096.9	1083.3	1067.2	1051.1	1035.4
0.1047	1202.4	1185.8	1168.9	1152.3	1134.7	1118.5	1102.5	1086.0	1072.3	1056.1	1039.7
0.2776	1220.4	1203.0	1187.4	1170.8	1154.7	1138.2	1121.5	1106.2	1090.3	1074.8	1058.3
0.4024	1228.8	1214.1	1198.4	1182.6	1165.8	1149.0	1132.5	1116.1	1099.9	1083.3	1067.5
0.4555	1237.0	1222.1	1204.7	1188.5	1172.6	1155.9	1139.1	1122.4	1105.5	1089.9	1076.2
0.6276	1253.3	1235.6	1219.1	1203.0	1187.3	1171.1	1155.5	1139.5	1123.8	1108.0	1093.5
0.7820	1270.9	1254.4	1238.3	1221.6	1205.7	1188.8	1172.9	1157.4	1140.7	1124.4	1108.6
0.8810	1274.9	1257.8	1241.0	1225.4	1212.0	1195.8	1179.3	1163.7	1147.3	1131.9	1115.5
0.9116	1279.9	1263.2	1247.8	1231.2	1215.2	1198.8	1182.3	1165.8	1150.2	1134.0	1119.3
1.004	1293.4	1277.2	1261.1	1245.4	1229.3	1212.9	1196.9	1180.7	1164.5	1148.2	1133.8
1.259	1315.8	1298.8	1282.7	1266.8	1250.2	1232.2	1219.1	1200.0	1183.5	1167.6	1151.8
1.492	1340.4	1324.8	1308.1	1292.2	1275.7	1259.5	1243.0	1227.0	1210.2	1193.9	1177.5
1.710	1360.5	1343.7	1327.3	1311.9	1295.5	1279.9	1263.7	1247.8	1231.4	1216.4	1199.0
1.875	1368.6	1352.5	1335.4	1320.1	1304.0	1288.1	1272.7	1256.6	1240.4	1225.2	1209.5
						$Mg(ClO_4)_2$					
0.0542	1195.2		1162.7		1128.4	1111.3	1094.8		1062.7		
0.0780	1201.1		1167.8		1134.9	1119.1	1101.6		1069.7		
0.0925	1203.6		1170.8		1137.7	1121.2	1104.6		1072.7		
0.1673	1212.8		1178.9		1146.0	1129.8	1114.0		1082.2		
0.2872	1226.0		1193.9		1161.8	1145.7	1129.8		1098.9		
0.3228	1230.6		1197.5		1165.4	1149.1	1133.5		1102.5		
0.4313	1245.5		1213.2		1181.4	1165.2	1147.0		1115.5		
0.6444	1268.2		1236.8		1205.9	1189.2	1173.3		1141.6		
1.059	1308.9		1278.5		1247.5	1232.0	1217.0		1185.5		
1.395	1342.5		1313.4		1282.1	1267.7	1253.3		1224.6		
1.717	1366.9		1336.5		1307.5	1293.2	1277.6		1249.9		
2.000	1385.5		1358.1		1329.1	1314.4	1301.6		1273.8		

form of the density equation, $\rho = a - b(T/\mathrm{K} - 273.15)$. Figure 1 displays the density isotherms at 298.15 K for all three salt solutions. However, there does not appear to be any literature data.

Ultrasonic Velocity. The measured ultrasonic velocities for methanolic $Mg(OAc)_2$, $Mg(NO_3)_2$, and $Mg(ClO_4)_2$ solutions are presented in Table 2 as functions of concentration and temperature. The densities and ultrasonic velocities were used to calculate the isentropic compressibilities ($\kappa_s = 1/u^2\rho$), and the κ_s vs concentration isotherms at three temperatures for these three methanolic systems are illustrated in Figure 2. Note that

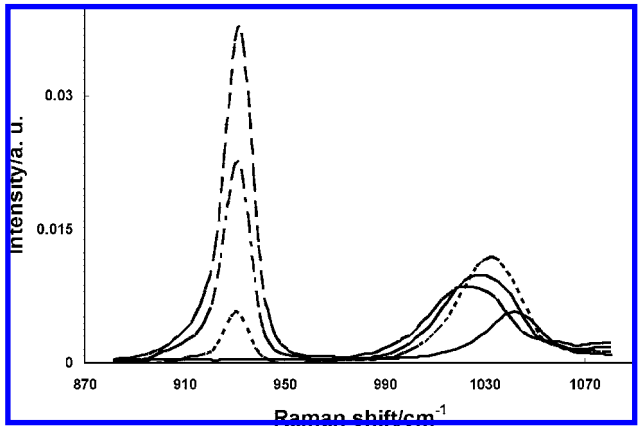

Figure 5. Raman spectra of methanolic $Mg(ClO_4)_2$ solutions corresponding to ν_1 (ClO_4) and ν_{C-O} (CH_3OH) bands. —, methanol; - - -, 0.2019 mol·kg^{-1}; — - —, 1.023 mol·kg^{-1}; — — —, 2.101 mol·kg^{-1}.

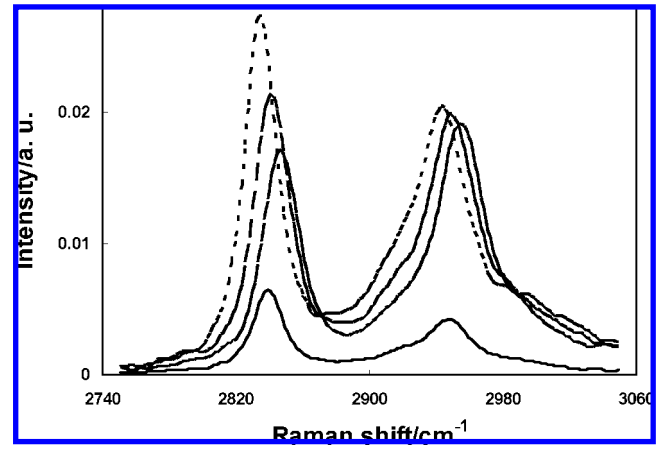

Figure 6. Raman spectra of methanolic $Mg(ClO_4)_2$ solutions corresponding to ν_{C-H} (CH_3OH) bands. —, methanol; - - -, 0.2019 mol·kg^{-1}; — - —, 1.023 mol·kg^{-1}; — — —, 2.101 mol·kg^{-1}.

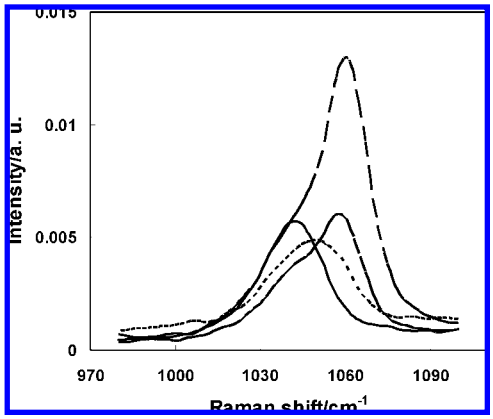

Figure 7. Raman spectra of methanolic $Mg(NO_3)_2$ solutions corresponding to ν_1 (NO_3^-) and ν_{C-O} (CH_3OH) bands. −, methanol; - - -, 0.2776 mol·kg^{-1}; − - −, 1.012 mol·kg^{-1}; − − −, 1.948 mol·kg^{-1}.

Table 3. Values of the Parameters of Equation 1 for Methanolic $Mg(OAc)_2$, $Mg(NO_3)_2$, and $Mg(ClO_4)_2$ Solutions

parameters	T/K = 273.15	T/K = 298.15	T/K = 313.15
	$Mg(OAc)_2$		
$10^{10}a_1$/Pa^{-1}	8.779	10.45	11.74
$10^{10}b_1$/Pa^{-1}·kg·mol^{-1}	−8.781	−5.002	−36.63
$10^{10}c_1$/Pa^{-1}·kg$^{1.5}$·mol$^{-1.5}$	58.58	54.86	304.4
$10^{10}d_1$/Pa^{-1}·kg^2·mol^{-2}	−199.0	−305.5	−1055.0
$10^{10}e_1$/Pa^{-1}·kg$^{2.5}$·mol$^{-2.5}$	318.6	654.0	1647.0
$10^{10}f_1$/Pa^{-1}·kg^3·mol^{-3}	−192.9	−473.4	−959.8
$10^{10}\sigma$/Pa^{-1}	0.013	0.018	0.016
	$Mg(NO_3)_2$		
$10^{10}a_1$/Pa^{-1}	8.757	10.338	11.54
$10^{10}b_1$/Pa^{-1}·kg·mol^{-1}	−5.272	−2.918	−5.875
$10^{10}c_1$/Pa^{-1}·kg$^{1.5}$·mol$^{-1.5}$	7.610	−4.189	5.692
$10^{10}d_1$ /Pa^{-1}·kg^2·mol^{-2}	−6.673	11.03	−3.727
$10^{10}e_1$/Pa^{-1}·kg$^{2.5}$·mol$^{-2.5}$	2.176	−9.313	0.500
$10^{10}f_1$ /Pa^{-1}·kg^3·mol^{-3}	−0.002	2.757	0.360
$10^{10}\sigma$/Pa^{-1}	0.035	0.036	0.044
	$Mg(ClO_4)_2$		
$10^{10}a_1$/Pa^{-1}	8.667	10.28	11.50
$10^{10}b_1$/Pa^{-1}·kg·mol^{-1}	−3.226	−2.629	−4.733
$10^{10}c_1$/Pa^{-1}·kg$^{1.5}$·mol$^{-1.5}$	1.212	−3.804	0.836
$10^{10}d_1$/Pa^{-1}·kg^2·mol^{-2}	−2.455	3.954	−1.569
$10^{10}e_1$/Pa^{-1}·kg$^{2.5}$·mol$^{-2.5}$	3.052	−0.121	3.009
$10^{10}f_1$/Pa^{-1}·kg^3·mol^{-3}	−1.006	−0.460	−1.123
$10^{10}\sigma$/Pa^{-1}	0.025	0.041	0.047

the solubility of $Mg(OAc)_2$ in methanol is low, and the measurements were performed up to 0.3042 mol·kg^{-1}. Isentropic compressibilities, κ_s, were fitted to an empirical equation[30,31]

$$\kappa_s = a_1 + b_1 m + c_1 m^{1.5} + d_1 m^2 + e_1 m^{2.5} + f_1 m^3 \qquad (1)$$

where a_1, b_1, c_1, d_1, e_1, and f_1 are temperature-dependent parameters and m is the concentration in mol·kg^{-1}. The numerical values of these parameters are shown in Table 3.

Apparently, the three solutes in methanol cause a decrease in compressibility as the salt concentration increases. The decreasing trend is roughly proportional to the ion−solvent interactions at a particular temperature. At a fixed temperature and concentration, e.g., 0.3 mol·kg^{-1}, methanolic $Mg(OAc)_2$ solution is more compressible than $Mg(NO_3)_2$, which in turn is more compressible than that of $Mg(ClO_4)_2$ solution. In contrast, aqueous $Mg(OAc)_2$ is less compressible than aqueous $Mg(NO_3)_2$.[22] It implies that the solvation structures of these two salts in water and methanol media are different which should be the case as water has three-dimensional network structure in contrast to methanol. The present isentropic compressibility results suggest the following sequence of anion−solvent interaction in methanol: OAc^- < NO_3^- < ClO_4^-. The observed trend could not be explained in terms of charge density of the ions as ionic radii, $r(OAc^-) = 2.32$ Å > $r(NO_3^-) = 1.79$ Å < $r(ClO_4^-) = 2.36$ Å.[32] The observed anion−solvent interactions are probably connected to the disparity in structure and chemical characteristics of the anions. For example, from OAc^- ($CH_3CO_2^-$) to NO_3^- to ClO_4^-, the number of oxygen atoms (interactive sites with methanol) is increasing in sequence though their integral charge is one. Furthermore, the influence of the hydrophobic CH_3 group in OAc^- is obviously prominent. Nevertheless, the observed trend of the anionic effects on the isentropic compressibility behavior appears to follow the Hofmeister series[33] as reported in aqueous solutions.[22] The OAc^- is at the salting-out side; NO_3^- is at the middle; and ClO_4^- is at the salt-in side of the series. Accordingly, these ions interact quite differently with the solvent molecules.

Electrical Conductivity. The experimental electrical conductivities for methanolic $Mg(OAc)_2$, $Mg(NO_3)_2$, and $Mg(ClO_4)_2$ solutions are listed in Table 4 as functions of concentration and temperature. Our conductivity data agree within ± 5 % with the literature values at 298.15 K.[27] Figure 3 shows that specific conductivity increases with increasing concentration and temperature for each system. At a particular concentration and temperature, the conductivities also follow the similar sequence, which was implied in the compressibility behavior. In other words, mobility of the solvated anions follows the sequence OAc^- < NO_3^- < ClO_4^- as the cation is common. Thus, the conductivity behavior of these salt solutions in methanol is also consistent with the Hofmeister series.[33]

The conductivity data over the whole concentration ranges were fitted to the Casteel−Amis equation[34,35]

$$\kappa = \kappa_{max}(m/\mu)^a \exp[b(m-\mu)^2 - a(m-\mu)/\mu] \qquad (2)$$

where μ is the concentration corresponding to the maximum conductivity, κ_{max}, at a given temperature; a and b are empirical parameters; and m is molality in mol·kg^{-1}. The least-squares fitted values of the parameters of eq 2 are summarized in Table 5. It is also apparent from Figure 3 that the κ vs m isotherms for $Mg(NO_3)_2$ solutions pass through a maximum at (1.179 ± 0.014, 1.448 ± 0.028, and 1.609 ± 0.041) mol·kg^{-1} at (273.15, 298.15, and 313.15) K, respectively, and thus the maxima show a positive shift with temperature. The appearance of maxima is the consequence of the competition between increasing charge carrier and decreasing mobility of the ions with increasing salt concentration.[36] The decreasing ionic mobility at higher concentrations is mainly because of a decrease of solution viscosity and ion association with an increase in temperature. Thus, the conductivity pattern suggests some kind of ion association in $Mg(NO_3)_2$ solutions at high concentrations. Such a behavior for $Mg(ClO_4)_2$ seems to be absent within the temperature and concentration ranges of this study. On the other hand, the conductivity values for methanolic $Mg(OAc)_2$ solutions are very low, reflecting less tendency to dissociate or/and greater association of Mg^{2+} with OAc^- than with NO_3^- and ClO_4^- in methanol and is consistent with the former two systems in an aqueous medium.[22]

Viscosity. The measured viscosities for methanolic solutions of $Mg(OAc)_2$, $Mg(NO_3)_2$, and $Mg(ClO_4)_2$ are collected in Table 6 at different concentrations and temperatures. The viscosity data for all the three systems are plotted in Figure 4 at two temperatures. A semiempirical equation

$$\eta = a_0 \exp(b_0 m + c_0 m^2) \qquad (3)$$

where a_0, b_0, and c_0 are the adjustable temperature-dependent parameters has been shown to be useful for data fitting over

Table 4. Electrical Conductivity, κ/S·m^{-1}, of Methanolic $Mg(OAc)_2$, $Mg(NO_3)_2$, and $Mg(ClO_4)_2$ Solutions as Functions of Concentration and Temperature

m	T/K								
mol·kg^{-1}	273.15	278.15	283.15	288.15	293.15	298.15	303.15	308.15	313.15
					$Mg(OAc)_2$				
0.0059	0.0325	0.0329	0.0334	0.0341	0.0349	0.0355	0.0362	0.0369	0.0376
0.0093	0.0550	0.0556	0.0562	0.0566	0.0575	0.0580	0.0586	0.0592	0.0598
0.0180	0.0621	0.0627	0.0634	0.0642	0.0649	0.0656	0.0665	0.0674	0.0685
0.0339	0.0796	0.0807	0.0818	0.0831	0.0843	0.0856	0.0868	0.0879	0.0890
0.0530	0.0922	0.0937	0.0954	0.0969	0.0985	0.1000	0.1018	0.1030	0.1041
0.0646	0.0965	0.0989	0.1008	0.1033	0.1055	0.1080	0.1103	0.1120	0.1137
0.0855	0.1060	0.1084	0.1089	0.1114	0.1149	0.1183	0.1220	0.1232	0.1243
0.1024	0.1148	0.1174	0.1198	0.1227	0.1258	0.1284	0.1302	0.1326	0.1348
0.1402	0.1289	0.1326	0.1355	0.1390	0.1426	0.1458	0.1487	0.1510	0.1535
0.1455	0.1307	0.1350	0.1388	0.1428	0.1463	0.1485	0.1524	0.1557	0.1577
0.1837	0.1414	0.1448	0.1465	0.1496	0.1536	0.1578	0.1617	0.1631	0.1660
0.2422	0.1507	0.1530	0.1656	0.1673	0.1693	0.1717	0.1746	0.1782	0.1817
0.2889	0.1565	0.1605	0.1642	0.1692	0.1735	0.1776	0.1810	0.1835	0.1868
					$Mg(NO_3)_2$				
0.0082	0.1095	0.1165	0.1221	0.1281	0.1341	0.1401	0.1462	0.1518	0.1573
0.0545	0.3036	0.3210	0.3368	0.3616	0.3807	0.3953	0.4108	0.4242	0.4382
0.0667	0.3337	0.3538	0.3738	0.3930	0.4120	0.4305	0.4481	0.4649	0.4799
0.1047	0.4393	0.4655	0.4908	0.5164	0.5415	0.5657	0.5889	0.6114	0.6326
0.2776	0.8097	0.8637	0.9168	0.9691	1.021	1.073	1.123	1.172	1.215
0.4024	1.002	1.073	1.143	1.214	1.277	1.343	1.410	1.476	1.537
0.4555	1.043	1.117	1.192	1.267	1.341	1.416	1.489	1.559	1.625
0.6276	1.207	1.300	1.394	1.489	1.584	1.680	1.775	1.867	1.951
0.7820	1.310	1.417	1.528	1.639	1.752	1.866	1.979	2.089	2.183
0.8810	1.334	1.447	1.561	1.678	1.797	1.918	2.037	2.154	2.262
0.9116	1.344	1.459	1.573	1.690	1.811	1.933	2.054	2.173	2.287
1.004	1.372	1.494	1.618	1.744	1.873	2.005	2.136	2.266	2.390
1.259	1.361	1.494	1.632	1.772	1.917	2.065	2.213	2.359	2.502
1.492	1.314	1.453	1.597	1.746	1.900	2.060	2.223	2.396	2.545
1.710	1.281	1.436	1.590	1.738	1.902	2.073	2.246	2.421	2.587
1.875	1.238	1.383	1.538	1.698	1.866	2.039	2.217	2.395	2.567
					$Mg(ClO_4)_2$				
0.0542	0.2699		0.3054		0.3414	0.3599	0.3785		0.4141
0.0780	0.4031		0.4563		0.5074	0.5344	0.5625		0.6138
0.0925	0.4435		0.5023		0.5615	0.5917	0.6223		0.6801
0.1673	0.6702		0.7619		0.8540	0.9009	0.9485		1.040
0.2872	0.9762		1.116		1.253	1.332	1.407		1.549
0.3228	1.058		1.213		1.370	1.452	1.534		1.691
0.4313	1.299		1.497		1.702	1.807	1.913		2.119
0.6444	1.752		2.001		2.209	2.389	2.541		2.844
1.059	2.122		2.513		2.926	3.143	3.367		3.813
1.395	2.273		2.731		3.221	3.480	3.746		4.297
1.717	2.343		2.848		3.390	3.683	3.979		4.592
2.000	2.355		2.892		3.474	3.779	4.100		4.750

Table 5. Least-Squares Fitted Values of the Parameters of Equation 2 for $Mg(OAc)_2$, $Mg(NO_3)_2$, and $Mg(ClO_4)_2$ Solutions at Different Temperatures

T	κ_{max}	μ		$10^{-3}b$	std dev
K	S·m^{-1}	mol·kg^{-1}	a	kg^2·mol^{-2}	in κ/S·m^{-1}
			$Mg(OAc)_2$		
273.15	0.1721	0.6043	0.4106	−0.0301	0.0028
298.15	0.1862	0.4330	0.4286	−0.6615	0.0023
313.15	0.1916	0.3731	0.4210	−1.402	0.0024
			$Mg(NO_3)_2$		
273.15	1.375	1.179	0.6884	−0.0617	0.0149
298.15	2.096	1.448	0.6907	−0.0561	0.0210
313.15	2.585	1.609	0.6918	−0.0572	0.0224
			$Mg(ClO_4)_2$		
273.15	2.351	1.680	0.8113	−0.0485	0.0347
298.15	3.733	1.937	0.7964	−0.0627	0.0362
313.15	4.707	2.053	0.8071	−0.0635	0.0431

wide concentration ranges.[31,37] It is apparent from Table 7 and Figure 4 that eq 3 adequately fits the viscosity data of methanolic $Mg(OAc)_2$, $Mg(NO_3)_2$, and $Mg(ClO_4)_2$ systems. Evidently, the viscosity values for all the solutes increases as the molality increases. At a fixed molality and temperature, $Mg(NO_3)_2$ solutions are more viscous than $Mg(OAc)_2$ or $Mg(ClO_4)_2$ solutions. With decreasing temperatures, the increasing trend of viscosity becomes exponential and is more pronounced for $Mg(NO_3)_2$ solutions. We conclude that viscosity data support the conductivity patterns for $Mg(NO_3)_2$ and $Mg(ClO_4)_2$ systems convincingly and signal the presence of some ion pairing in $Mg(NO_3)_2$ solutions at high concentrations.

FT-Raman Spectra. To get a clear picture of anion−solvent interactions and ion pairing, FT-Raman spectra were recorded for all the methanolic salt solutions and are displayed in Figures 5 to 10. Considering the probable ion−solvent and ion−ion interactions, Raman spectra are focused in the ν_1 for NO_3^- and ClO_4^-, ν_{C-O} and ν_{C-H} regions, and the relevant band parameters are summarized in Table 8. The measured band frequencies are in good agreement with the literature values for pure methanol[38] and methanolic $Mg(ClO_4)_2$ solutions.[39,40]

The ν_{C-O} mode for pure methanol shows a sharp band at 1042 cm^{-1}, which gets red-shifted with the addition of Mg salts. For $Mg(ClO_4)_2$ solutions, the shift is large ($\Delta\nu$ = 19 cm^{-1}) compared to $Mg(NO_3)_2$ ($\Delta\nu$ = 8 cm^{-1}) solutions, while almost equal amounts ($\approx$2 m) of ions were added to methanol. This suggests that the ClO_4^- ion (with four oxygen) gets more

Table 6. Viscosity, η/mPa·s, of Methanolic $Mg(OAc)_2$, $Mg(NO_3)_2$, and $Mg(ClO_4)_2$ Solutions at Various Concentrations and Temperatures

m	T/K								
mol·kg^{-1}	273.15	278.15	283.15	288.15	293.15	298.15	303.15	308.15	313.15
					$Mg(OAc)_2$				
0.0140	0.8210	0.7547	0.6979	0.6458	0.6000	0.5583	0.5207	0.4859	0.4545
0.0180	0.8229	0.7565	0.6998	0.6478	0.6022	0.5605	0.5223	0.4878	0.4559
0.0339	0.8417	0.7732	0.7143	0.6606	0.6132	0.5703	0.5306	0.4960	0.4632
0.0646	0.8642	0.7927	0.7304	0.6743	0.6249	0.5802	0.5393	0.5027	0.4698
0.1012	0.9108	0.8332	0.7669	0.7063	0.6535	0.6059	0.5622	0.5234	0.4881
0.1300	0.9308	0.8509	0.7824	0.7206	0.6660	0.6170	0.5718	0.5320	0.4956
0.1402	0.9493	0.8670	0.7965	0.7286	0.6731	0.6234	0.5779	0.5368	0.5000
0.1700	0.9637	0.8812	0.8105	0.7465	0.6902	0.6396	0.5933	0.5518	0.5145
0.2003	0.9889	0.9025	0.8289	0.7639	0.7039	0.6529	0.6048	0.5625	0.5239
0.2422	1.042	0.9469	0.8664	0.7865	0.7255	0.6701	0.6232	0.5782	0.5375
0.2453	1.036	0.9437	0.8643	0.7929	0.7305	0.6746	0.6232	0.5780	0.5373
0.2889	1.091	0.9892	0.8961	0.8205	0.7548	0.6956	0.6420	0.5942	0.5513
					$Mg(NO_3)_2$				
0.0082	0.8298	0.7627	0.7006	0.6479	0.6014	0.5595	0.5215	0.4860	0.4543
0.0545	0.8885	0.8108	0.7465	0.6900	0.6412	0.5957	0.5545	0.5169	0.4830
0.0667	0.9109	0.8360	0.7750	0.7149	0.6621	0.6148	0.5716	0.5321	0.4662
0.1047	0.9548	0.8755	0.8049	0.7430	0.6872	0.6361	0.5909	0.5501	0.5128
0.2776	1.129	1.029	0.9437	0.8665	0.7989	0.7381	0.6836	0.6334	0.5885
0.4024	1.336	1.213	1.109	1.016	0.9313	0.8609	0.7943	0.7332	0.6799
0.4555	1.400	1.273	1.158	1.060	0.9778	0.8966	0.8264	0.7633	0.7062
0.6276	1.836	1.732	1.562	1.408	1.271	1.146	1.050	0.9449	0.8707
0.7820	2.128	1.905	1.719	1.556	1.415	1.287	1.177	1.077	0.9902
0.8810	2.180	1.938	1.743	1.575	1.429	1.301	1.184	1.083	0.9936
0.9116	2.329	2.079	1.866	1.679	1.517	1.369	1.245	1.135	1.038
1.004	2.559	2.278	2.041	1.828	1.650	1.491	1.354	1.233	1.124
1.259	3.717	3.260	2.891	2.586	2.306	2.078	1.875	1.694	1.536
1.492	4.748	4.119	3.619	3.198	2.833	2.541	2.267	2.044	1.837
1.710	6.086	5.244	4.554	3.978	3.500	3.094	2.730	2.433	2.169
1.875	7.175	6.178	5.339	4.642	4.058	3.556	3.138	2.765	2.450
					$Mg(ClO_4)_2$				
0.0542	0.8742		0.7345		0.6286	0.5841	0.5431		0.4735
0.0925	0.9094		0.7680		0.6569	0.6098	0.5669		0.4938
0.1673	0.9874		0.8318		0.7098	0.6560	0.6084		0.5284
0.2872	1.130		0.9437		0.7995	0.7391	0.6840		0.5874
0.3228	1.168		0.9745		0.8248	0.7618	0.7005		0.6082
0.4313	1.329		1.102		0.9286	0.8560	0.7937		0.6824
0.6444	1.640		1.342		1.112	1.019	0.9348		0.7966
1.059	2.393		1.928		1.585	1.446	1.323		1.119
1.395	3.292		2.608		2.110	1.910	1.732		1.445
1.717	3.854		3.023		2.430	2.196	1.990		1.656
2.000	4.766		3.682		2.923	2.624	2.362		1.945

Table 7. Least-Squares Parameters of Equation 3 for Methanolic $Mg(OAc)_2$, $Mg(NO_3)_2$, and $Mg(ClO_4)_2$ Solutions

T/K	a_0/mPa·s	b_0	c_0	std dev in η/mPa·s
		$Mg(OAc)_2$		
273.15	0.8095	1.108	−0.3158	0.0064
313.15	0.4486	0.8615	−0.4944	0.0018
		$Mg(NO_3)_2$		
273.15	0.8205	1.240	−0.0427	0.0652
313.15	0.4468	1.0696	−0.8554	0.0281
		$Mg(ClO_4)_2$		
273.15	0.8144	1.196	−0.1585	0.0636
313.15	0.4447	1.034	−0.1497	0.0198

strongly solvated than NO_3^- (three oxygen) in methanol as discussed in the preceding sections. On the other hand, the addition of $Mg(OAc)_2$ could not effect any change in the position of the ν_{C-O} band of methanol up to its permitted solubility. Similar band shifting patterns were also observed in the CH_3 symmetric stretching (ν_{C-H}) region of methanol. Here the shifting is distributed over two sharp bands (Fermi resonance doublet)[39] at 2839 cm^{-1} and 2947 cm^{-1}. The $Mg(OAc)_2$ could not produce any impact at ν_{C-H} bands. The addition of $Mg(ClO_4)_2$ and $Mg(NO_3)_2$ salts blue-shifted the ν_{C-H} bands to almost equal extent ($\Delta\nu = \approx 8$ cm^{-1}). However, the shifting pattern in $Mg(ClO_4)_2$ solutions was not straightforward. Both the (2839 and 2947) cm^{-1} bands of methanol first exhibited a red shift followed by a blue shift with increasing salt concentration until saturation. Hence the observed patterns of ν_{C-O} and ν_{C-H} bands confirm that $Mg(OAc)_2$ has very little effect on methanol structure,[41] while $Mg(ClO_4)_2$ interacts much more

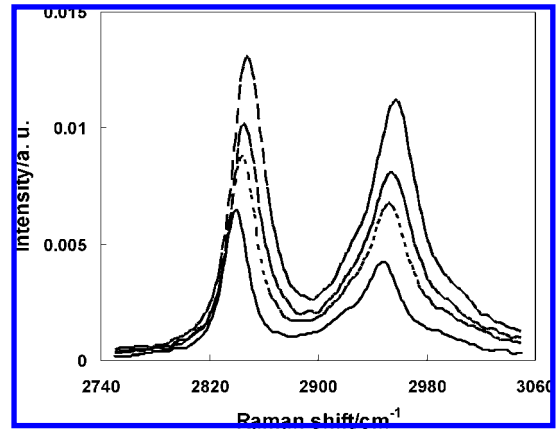

Figure 8. Raman spectra of methanolic $Mg(NO_3)_2$ solutions corresponding to ν_{C-H} (CH_3OH) bands. −, methanol; - - -, 0.2776 mol·kg^{-1}; − - −, 1.012 mol·kg^{-1}; − − −, 1.948 mol·kg^{-1}.

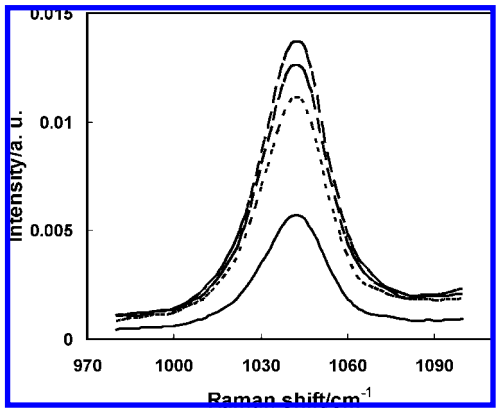

Figure 9. Raman spectra of methanolic $Mg(OAc)_2$ solutions corresponding to ν_{C-O} (CH_3OH) bands. −, methanol; - - -, 0.0901 mol·kg^{-1}; − - −, 0.2668 mol·kg^{-1}; − − −, 0.3655 mol·kg^{-1}.

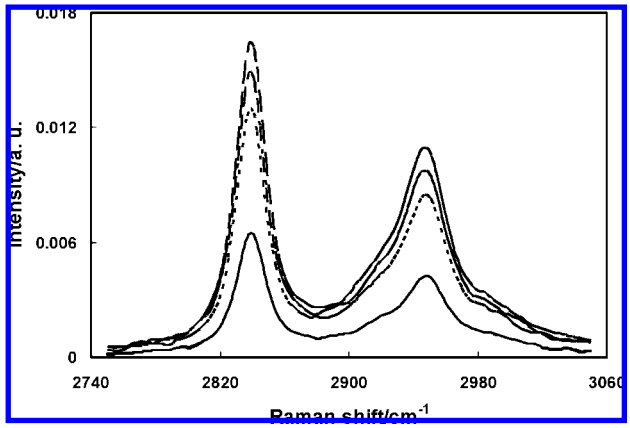

Figure 10. Raman spectra of methanolic $Mg(OAc)_2$ solutions corresponding to ν_{C-H} (CH_3OH) bands. −, methanol; - - -, 0.0901 mol·kg^{-1}; − - −, 0.2668 mol·kg^{-1}; − − −, 0.3655 mol·kg^{-1}.

Table 8. Assignments of Modes and Peak Positions in the Raman Spectra of Methanolic $Mg(ClO_4)_2$, $Mg(NO_3)_2$, and $Mg(OAc)_2$ Solutions

peak positions/cm^{-1}				
$Mg(ClO_4)_2$				
m/mol·kg^{-1}	ν_1 (ClO_4)	ν_{C-O} (CH_3OH)	ν_{C-H} (CH_3OH)	
pure methanol		1042	2839	2947
0.2019	930	1032	2835	2943
1.023	932	1028	2841	2949
2.101	932	1023	2847	2955
$Mg(NO_3)_2$				
	ν_1 (NO_3)	ν_{C-O} (CH_3OH)	ν_{C-H} (CH_3OH)	
pure methanol		1042	2839	2947
0.2776			2844	2953
1.012	1057	1037	2846	2955
1.948	1060	1034	2847	2957
$Mg(OAc)_2$				
		ν_{C-O} (CH_3OH)	ν_{C-H} (CH_3OH)	
pure methanol		1042	2839	2947
0.0901		1042	2839	2947
0.2668		1042	2839	2947
0.3655		1042	2839	2947

strongly with solvent than $Mg(NO_3)_2$, indicating the possibility of strong ion−ion interaction in $Mg(NO_3)_2$ solutions.

The ν_1 band for ClO_4^- and NO_3^- showed a small blue shift with increasing salt concentration in methanol. In the case of $Mg(ClO_4)_2$ solutions, the shift was ≈2 cm^{-1} up to saturation and indicates the absence of any ion pairing between Mg^{2+} and ClO_4^-. In $Mg(NO_3)_2$ solutions (Figure 7), the ν_1 and ν_{C-O} bands overlapped at low concentration (0.2776 m) resulting in a broadband centered at ≈1050 cm^{-1}, and their individual band positions could not be determined without deconvolution. At higher concentrations, however, both the bands separated out with clear shoulders for the ν_{C-O} band. At 1.012 m, the ν_1 band appeared at 1057 cm^{-1} and shifted to 1060 cm^{-1} at 1.948 m. Therefore, an apparent blue shift of ≈3 cm^{-1} from (≈1 to 2) m for the ν_1 band in $Mg(NO_3)_2$ solutions could be ascribed to the presence of some solvent-shared ion pairing beyond ≈1 m and corroborate the conductivity and viscosity behavior.

Conclusions

Anionic charge density is not the governing factor for explaining the isentropic compressibility of methanolic $Mg(OAc)_2$, $Mg(NO_3)_2$, and $Mg(ClO_4)_2$ solutions; however, the Hofmeister effect is observed in these solutions. The observed patterns of ν_{C-O} and ν_{C-H} bands confirm that $Mg(OAc)_2$ has very little effect on methanol structure, while $Mg(ClO_4)_2$ interacts much more strongly with methanol than $Mg(NO_3)_2$.

Acknowledgment

The paper is dedicated to Dr. Robin H. Stokes on the occasion of his 90th birthday. The authors (A.W. and S.M.) are grateful to the Director, North-East Institute of Science and Technology, CSIR, Jorhat - 785 006, Assam, India, for interest in this work, and A.W. is thankful to the Council of Scientific and Industrial Research, New Delhi, India, for the award of senior research fellowship. The authors are also grateful to the Sophisticated Analytical Instrumentation Facility (SAIF), Indian Institute of Technology-Madras, India, for recording the Raman spectra. We thank anonymous reviewers for several valuable suggestions.

Supporting Information Available:

Table 1S. This material is available free of charge via the Internet at http://pubs.acs.org.

Literature Cited

(1) Robinson, R. A.; Stokes, R. H. *Electrolyte Solutions*, 2nd ed.; revised; Butterworth: London, 1965.
(2) Harned, H. S.; Owen, B. B. *The Physical Chemistry of Electrolytic Solutions*, 3rd ed.; Reinhold: New York, 1958.
(3) Monk, C. B. *Electrolytic Dissociation*; Academic Press: London, 1961.
(4) Davies, C. W. *Ion Association*; Butterworth: London, 1962.
(5) Nancollas, G. H. *Interactions in Electrolyte Solutions*; Elsevier: Amsterdam, 1966.
(6) Marcus, Y. *Ion Solvation*; Wiley: Chichester, U.K., 1986.
(7) Barthel, J. M. G.; Krienke, H.; Kunz, W. *Physical Chemistry of Electrolyte Solutions: Modern Aspect*; Steinkopf: Darmstadt, 1998.
(8) Covington, A. K., Dickinson, T., Eds. *Physical Chemistry of Organic Solvent Systems*; Plenum Press: London, 1973.
(9) Popovych, O.; Tomkins, R. P. T. *Nonaqueous Solution Chemistry*; Wiley: New York, 1981.
(10) Burgesss, J. *Metal Ions in Solution*; Ellis Horwood: New York, 1978.
(11) Magini, M.; Licheri, G.; Paschina, G.; Piccaluga, G.; Pinna, G. *X-ray Diffraction of Ions in Aqueous Solutions: Hydration and Complex Formation*; CRC Press: Boca Raton, FL, 1988.
(12) Conway, B. E. *Ionic Hydration in Chemistry and Biophysics, Studies in Physical and Theoretical Chemistry 12*; Elsevier: Amsterdam, 1981.
(13) Hinton, J. F.; Amis, E. S. Nuclear Magnetic Resonance Studies of Ions in Pure and Mixed Solvents. *Chem. Rev.* **1967**, *67*, 367–425.
(14) Marcus, Y. Ionic Radii in Aqueous Solutions. *Chem. Rev.* **1988**, *88*, 1475–1498.
(15) Ohtaki, H.; Radnai, T. Structure and Dynamics of Hydrated Ions. *Chem. Rev.* **1993**, *93*, 1157–1204.
(16) Jenkins, H. D. B.; Marcus, Y. Viscosity B-Coefficients of Ions in Solution. *Chem. Rev.* **1995**, *95*, 2695–2724.
(17) Kalidas, C.; Hefter, G.; Marcus, Y. Gibbs Energies of Transfer of Cations from Water to Mixed Aqueous Organic Solvents. *Chem. Rev.* **2000**, *100*, 819–852.

(18) Hefter, G. T.; Marcus, Y.; Waghorne, W. E. Enthalpies and Entropies of Transfer of Electrolytes and Ions from Water to Mixed Aqueous Organic Solvents. *Chem. Rev.* **2002**, *102*, 2773–2836.
(19) Marcus, Y.; Hefter, G. Standard Partial Molar Volumes of Electrolytes and Ions in Nonaqueous Solvents. *Chem. Rev.* **2004**, *104*, 3405–3452.
(20) Marcus, Y.; Hefter, G. Ion Pairing. *Chem. Rev.* **2006**, *106*, 4585–4621.
(21) Smedley, S. I. *Interpretation of Ionic Conductivity in Liquids*; Plenum: New York, 1980.
(22) Wahab, A.; Mahiuddin, S.; Hefter, G.; Kunz, W.; Minofar, B.; Jungwirth, P. Ultrasonic Velocities, Densities, Viscosities, Electrical Conductivities, Raman Spectra, and Molecular Dynamics Simulations of Aqueous Solutions of $Mg(OAc)_2$ and $Mg(NO_3)_2$: Hofmeister Effects and Ion Pair Formation. *J. Phys. Chem. B* **2005**, *109*, 24108–24120.
(23) Kamarudin, S. K.; Daud, W. R. W.; Ho, S. L.; Hasran, U. A. Overview on the Challenges and Developments of Micro-Direct Methanol Fuel Cells (DMFC). *J. Power Sources* **2007**, *163*, 743–754.
(24) Wee, J.-H. Which Type of Fuel Cell is More Competitive for Portable Application: Direct Methanol Fuel Cells or Direct Borohydride Fuel Cells. *J. Power Sources* **2006**, *161*, 1–10.
(25) Whitacre, J. F.; Valdez, T.; Narayanan, S. R. Investigation of Direct Methanol Fuel Cell Electrocatalysts Using a Robust Combinatorial Technique. *J. Electrochem. Soc.* **2005**, *152*, A1780–A1789.
(26) Grossfield, A.; Ren, P.; Ponder, J. W. Ion Solvation Thermodynamics from Simulation with a Polarizable Force Field. *J. Am. Chem. Soc.* **2003**, *125*, 15671–15682.
(27) Rysselberghe, P. V.; Fristrom, R. M. The conductance of non-aqueous solutions of magnesium and calcium perchlorates. *J. Am. Chem. Soc.* **1945**, *67*, 680–682.
(28) Vogel, A. I. *A Textbook of Practical Organic Chemistry*, 3rd ed.; ELBS: Longman, U.K., 1975; p 268.
(29) Wu, Y. C.; Koch, W. F.; Pratt, K. W. Proposed New Electrolytic Conductivity Primary Standard for KCl Solutions. *J. Res. Natl. Inst. Stand. Technol.* **1991**, *96*, 191–201.
(30) Millero, F. J.; Ricco, J.; Schreiber, D. R. PVT properties of Concentrated Aqueous Electrolytes. II. Compressibilities and Apparent Molar Compressibilities of Aqueous NaCl, Na_2SO_4, $MgCl_2$, and $MgSO_4$ from Dilute Solution to Saturation and from 0 to 50 °C. *J. Solution Chem.* **1982**, *11*, 671–686.
(31) Wahab, A.; Mahiuddin, S.; Hefter, G.; Kunz, W. Densities, Ultrasonic Velocities, Viscosities, and Electrical Conductivities of Aqueous Solutions of $Mg(OAc)_2$ and $Mg(NO_3)_2$. *J. Chem. Eng. Data* **2006**, *51*, 1609–1616.
(32) Marcus, Y. *Ion Properties*; Marcel Dekker: New York, 1997.
(33) Hofmeister, F. *Naum-Schmiedebergs Archiv Expt. Pathol. Pharmakol.* **1888**, *23*, 247–260. English translation: Kunz, W.; Henle, J.; Ninham, B. W. 'Zur Lehre von der Wirkung der Salze' (about the science of the effect of salts): Franz Hofmeister's historical papers. *Curr. Opin. Colloid Interface Sci.* **2004**, *9*, 19–37.
(34) Casteel, J. F.; Amis, E. S. Specific Conductance of Concentrated Solutions of Magnesium Salts in Water-Ethanol System. *J. Chem. Eng. Data* **1972**, *17*, 55–59.
(35) Ding, M. S. Casteel-Amis Equation: Its Extension from Univariate to Multivariate and Its Use as a Two-Parameter Function. *J. Chem. Eng. Data* **2004**, *49*, 1469–1475.
(36) Bešter-Rogač, M. Electrical conductivity of concentrated aqueous solutions of divalent metal sulfates. *J. Chem. Eng. Data* **2008**, *53*, 1355–1359.
(37) Mahiuddin, S.; Ismail, K. Concentration Dependence of the Viscosity of Aqueous Electrolytes. A Probe into Higher Concentration. *J. Phys. Chem.* **1983**, *87*, 5241–5244.
(38) Kabisch, G.; Pollmer, K. Hydrogen bonding in methanol-organic solvent and methanol-water mixtures as studied by the ν_{CO} and ν_{OH}. *J. Mol. Struct.* **1982**, *81*, 35–50.
(39) Kabisch, G.; Bader, I.; Emons, H.-H.; Pollmer, K. A Raman spectroscopic investigation of the structure of magnesium salt solutions in methanol and methanol-water mixture. *J. Mol. Liq.* **1983**, *26*, 139–157.
(40) Minc, S.; Kurowski, S. Mutual interactions in solutions of polar substances as observed in the Raman effect-III.Methanol solutions of Li, Na, Mg, Ca and Ba perchlorate. *Spectrochim. Acta* **1963**, *19*, 339–344.
(41) Hidaka, F.; Yoshimura, Y.; Kanno, H. Anionic Effect on Raman OD Stretching Spectra for Alcoholic LiX Solutions (X = Cl, Br, I, ClO_4, NO_3, and CH_3COO). *J. Solution Chem.* **2003**, *32*, 239–251.

Received for review June 25, 2008. Accepted August 31, 2008.

JE800463K